

Analysis of a 1:2 Rectangular Waveguide Power Divider for Phased Array Application Using Multiple Cavity Modeling Technique

Debendra Kumar Panda and Ajay Chakraborty

IEEE, India

Abstract— A method of moment based analysis of the feed network of a waveguide fed two dimensional array antennas has been presented using Multi Cavity Modeling Technique (MCMT) in transmitting mode. The proposed power divider is unlikely to the family of Tees. The output ports are in the same planes as the input which is an advantage for phased array applications. The proposed 1:2 power divider has good agreement with the theory, CST microwave studio simulated and measured data over entire X-band frequency range.

1. INTRODUCTION

Low cost, Low Profile two dimensional scanning phased array antennas have wide application in Low Earth Orbit (LEO), Middle Earth Orbit (MEO) and Geostationary Earth Orbit (GEO) satellite communication. Multi-port Power divider has already found wide applications in phased array techniques. Basic requirements for the considered class of beam forming networks are: Low losses in the operational frequency band, the high accuracy of power splitting (With necessary amplitude and phase distribution at the outputs). Today, a large number of configurations and power divider constructions are known [1–6]. However the problems of theoretical analysis of high quality power divider remain unsolved. Effort has been made to miniaturize (dimensionally) a 1:2 power divider with wide band frequency response.

Present work was performed for theoretical analysis of a 1:2 power divider for phased array application using Multi Cavity Modeling Technique (MCMT) [7] and compared with the practical data. The technique involves in replacing all the apertures and discontinuities of the waveguide structures, with equivalent magnetic current densities so that the given structure can be analyzed using only Magnetic Field Integral Equation (MFIE). Since only the magnetic currents present in the apertures are considered the methodology involves only solving simple magnetic integral equation rather than the complex integral equation involving both the electric and magnetic current densities.

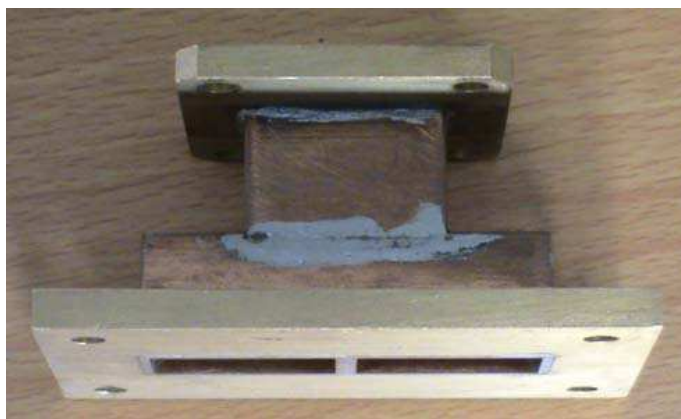


Figure 1: Photograph of a 1:2 power divider.

2. FORMULATION OF THEORY

The photograph of a basic 1:2 power divider is shown in Figure 1 and with its cavity modeling and details of region which shows that the structures have 3 waveguide regions and 1 cavity region shown in Figure 2. The interfacing apertures between different regions are replaced by equivalent magnetic current densities. The electric field at the aperture is assumed to be

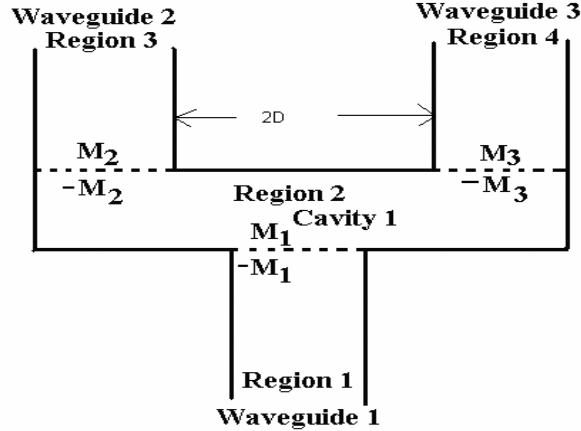


Figure 2: Cavity modeling and details of regions of a basic 1:2 power divider.

$$\vec{E} = \hat{u}_x \sum_{p=1}^M E_{px} e_{px} + \hat{u}_y \sum_{p=1}^M E_{py} e_{py} \quad (1)$$

where the basis function e_p ($p = 1, 2, 3, \dots, M$) are defined by

$$e_p^{i,y} = \begin{cases} \sin \left\{ \frac{p\pi}{2L} (x - x_w + L) \right\} & \text{for } x_w - L \leq x \leq x_w + L \\ 0 & \text{elsewhere} \end{cases} \quad (2a)$$

$$e_p^{i,x} = \begin{cases} \sin \left\{ \frac{p\pi}{2W} (y - y_w + W) \right\} & \text{for } y_w - W \leq y \leq y_w + W \\ 0 & \text{elsewhere} \end{cases} \quad (2b)$$

In the above expressions:

- $L = a$, $W = b$, $x_w = 0$ and $y_w = 0$ for aperture 1, aperture 2 and aperture 3 with respect to waveguide co-ordinate.
- $L = a$, $W = b$, $x_w = 0$ and $y_w = 0$ for aperture 1 with respect to cavity axis.
- $L = a$, $W = b$, $x_w = D + a$ and $y_w = 0$ for aperture 2 with respect to cavity axis.
- $L = a$, $W = b$, $x_w = D - a$ and $y_w = 0$ for aperture 3 with respect to cavity axis.
- where $a = 22.86$ mm, $b = 10.16$ mm, $D = 1.27$ mm.
- where $2D$ is the distance between waveguide-2 and waveguide-3.

The X -component of incident magnetic field at the aperture for the transmitting mode is a dominant TE_{10} mode and is given by

$$H_x^{inc} = -Y_0 \cos \left(\frac{\pi x}{2a} \right) e^{-j\beta z}$$

3. EVALUATION OF THE INTERNALLY SCATTERED FIELD

The internally scattered field is obtained by using the modal expansion approach presented in [8]. The internally scattered electric field is given in [9]. Once the electric field is obtained, the corresponding magnetic fields can be derived.

The modal voltages are given by (considering only $e_{pq}^{i,tn}$ part of the aperture electric field):

$$V_{mn}^e = \sqrt{2ab} [E_{px} - E_{py}] \quad (3)$$

$$V_{mn}^m = 0 \quad (4)$$

The x -component of internally scattered magnetic field can be obtained as,

$$H_x^{wvg} (E_p^i, y) = H_x^{wvg} (M_p^i, x) = \begin{cases} -\sum_{m=1}^{\infty} Y_{m0}^e \sin \left\{ \frac{m\pi}{2a} (x+a) \right\} & \text{for } p=m \text{ and } n=0 \\ 0 & \text{Otherwise} \end{cases} \quad (5)$$

$$H_x^{wvg} (E_p^i, x) = -H_x^{wvg} (M_p^i, y) = 0 \quad (6)$$

$$H_y^{wvg} (E_p^i, y) = H_y^{wvg} (M_p^i, x) = 0 \quad (7)$$

$$H_y^{wvg} (E_p^i, x) = -H_y^{wvg} (M_p^i, y) = \begin{cases} \sum_{n=0}^{\infty} Y_{0n}^e \sin \left\{ \frac{n\pi}{2b} (y+b) \right\} & \text{for } p=n \text{ and } m=0 \\ 0 & \text{Otherwise} \end{cases} \quad (8)$$

4. EVALUATION OF THE CAVITY SCATTERED FIELD

The tangential components of the cavity scattered fields are derived in [5]. The final form of the tangential components of the cavity scattered field will be same as given in [6], where L_c is the length and W_c is the width of the cavity. L_i and W_i are the half length and half width of i th aperture.

$$\begin{aligned} H_x^{cav^j} (M_i^x) &= -\frac{j\omega\varepsilon}{k^2} \sum_{m=1}^{\infty} \sum_{n=0}^{\infty} \frac{\varepsilon_m \varepsilon_n L_i W_i}{2L_c W_c} \left\{ k^2 - \left(\frac{m\pi}{2L_c} \right)^2 \right\} \sin \left\{ \frac{m\pi}{2L_c} (x+L_c) \right\} \\ &\times \cos \left\{ \frac{n\pi}{2W_c} (y+W_c) \right\} \cos \left\{ \frac{n\pi}{2W_c} (y_w+W_c) \right\} \sin c \left\{ \frac{n\pi}{2W_c} W_i \right\} F_x(p) \\ &\times \frac{(-1)}{\Gamma_{mn} \sin \{2\Gamma_{mn} t_c\}} \begin{cases} \cos \{ \Gamma_{mn} (z-t_c) \} \cos \{ \Gamma_{mn} (z_0+t_c) \} & z > z_0 \\ \cos \{ \Gamma_{mn} (z_0-t_c) \} \cos \{ \Gamma_{mn} (z+t_c) \} & z < z_0 \end{cases} \end{aligned} \quad (9)$$

$$\begin{aligned} H_x^{cav^j} (M_i^y) &= \frac{j\omega\varepsilon}{k^2} \sum_{m=1}^{\infty} \sum_{n=0}^{\infty} \frac{\varepsilon_m \varepsilon_n L_i W_i}{2L_c W_c} \frac{m\pi}{2L_c} \frac{n\pi}{2W_c} \sin \left\{ \frac{m\pi}{2L_c} (x+L_c) \right\} \\ &\times \cos \left\{ \frac{n\pi}{2W_c} (y+W_c) \right\} \cos \left\{ \frac{m\pi}{2L_c} (x_w+L_c) \right\} \sin c \left\{ \frac{m\pi}{2L_c} L_i \right\} F_y(p) \\ &\times \frac{(-1)}{\Gamma_{mn} \sin \{2\Gamma_{mn} t_c\}} \begin{cases} \cos \{ \Gamma_{mn} (z-t_c) \} \cos \{ \Gamma_{mn} (z_0+t_c) \} & z > z_0 \\ \cos \{ \Gamma_{mn} (z_0-t_c) \} \cos \{ \Gamma_{mn} (z+t_c) \} & z < z_0 \end{cases} \end{aligned} \quad (10)$$

$$\begin{aligned} H_y^{cav^j} (M_i^x) &= \frac{j\omega\varepsilon}{k^2} \sum_{m=1}^{\infty} \sum_{n=0}^{\infty} \frac{\varepsilon_m \varepsilon_n L_i W_i}{2L_c W_c} \frac{m\pi}{2L_c} \frac{n\pi}{2W_c} \cos \left\{ \frac{m\pi}{2L_c} (x+L_c) \right\} \\ &\times \sin \left\{ \frac{n\pi}{2W_c} (y+W_c) \right\} \cos \left\{ \frac{n\pi}{2W_c} (y_w+W_c) \right\} \sin c \left\{ \frac{n\pi}{2W_c} W_i \right\} F_x(p) \\ &\times \frac{(-1)}{\Gamma_{mn} \sin \{2\Gamma_{mn} t_c\}} \begin{cases} \cos \{ \Gamma_{mn} (z-t_c) \} \cos \{ \Gamma_{mn} (z_0+t_c) \} & z > z_0 \\ \cos \{ \Gamma_{mn} (z_0-t_c) \} \cos \{ \Gamma_{mn} (z+t_c) \} & z < z_0 \end{cases} \end{aligned} \quad (11)$$

$$\begin{aligned} H_y^{cav^j} (M_i^y) &= -\frac{j\omega\varepsilon}{k^2} \sum_{m=1}^{\infty} \sum_{n=0}^{\infty} \frac{\varepsilon_m \varepsilon_n L_i W_i}{2L_c W_c} \left\{ k^2 - \left(\frac{n\pi}{2W_c} \right)^2 \right\} \cos \left\{ \frac{m\pi}{2L_c} (x+L_c) \right\} \\ &\times \sin \left\{ \frac{n\pi}{2W_c} (y+W_c) \right\} \cos \left\{ \frac{m\pi}{2L_c} (x_w+L_c) \right\} \sin c \left\{ \frac{m\pi}{2L_c} L_i \right\} F_y(p) \\ &\times \frac{(-1)}{\Gamma_{mn} \sin \{2\Gamma_{mn} t_c\}} \begin{cases} \cos \{ \Gamma_{mn} (z-t_c) \} \cos \{ \Gamma_{mn} (z_0+t_c) \} & z > z_0 \\ \cos \{ \Gamma_{mn} (z_0-t_c) \} \cos \{ \Gamma_{mn} (z+t_c) \} & z < z_0 \end{cases} \end{aligned} \quad (12)$$

At the region of the window, the tangential component of the magnetic field in the aperture should be identical and applying the proper boundary conditions at the aperture the electric fields can be evaluated [6].

5. IMPOSITION OF THE BOUNDARY CONDITION

At the region of the window, the tangential component of the magnetic field in the aperture should be identical and is given by:

$$H_x^{wvg1}(M_1^x) + H_x^{cav}(M_1^x) + H_x^{wvg1}(M_1^y) + H_x^{cav}(M_1^y) - H_x^{cav}(M_2^x) - H_x^{cav}(M_2^y) - H_x^{cav}(M_3^x) - H_x^{cav}(M_3^y) = 2H_x^{inc} \quad (13)$$

$$H_y^{wvg1}(M_1^x) + H_y^{cav}(M_1^x) + H_y^{wvg1}(M_1^y) + H_y^{cav}(M_1^y) - H_y^{cav}(M_2^x) - H_y^{cav}(M_2^y) - H_y^{cav}(M_3^x) - H_y^{cav}(M_3^y) = 0 \quad (14)$$

$$-H_x^{cty}(M_1^x) - H_x^{cav}(M_1^y) + H_x^{cav}(M_2^x) + H_x^{wvg2}(M_2^x) + H_x^{cav}(M_2^y) + H_x^{wvg2}(M_2^y) + H_x^{cav}(M_3^x) + H_x^{cav}(M_3^y) = 0 \quad (15)$$

$$-H_y^{cav}(M_1^x) - H_y^{cav}(M_1^y) + H_y^{cav}(M_2^x) + H_y^{wvg2}(M_2^x) + H_y^{cav}(M_2^y) + H_x^{wvg2}(M_2^y) + H_y^{cav}(M_3^x) + H_y^{cav}(M_3^y) = 0 \quad (16)$$

$$-H_x^{cav}(M_1^x) - H_x^{cav}(M_1^y) + H_x^{cav}(M_2^x) + H_x^{cav}(M_2^y) + H_x^{cav}(M_3^x) + H_x^{wvg3}(M_2^x) + H_x^{cav}(M_3^y) + H_x^{wvg3}(M_3^y) = 0 \quad (17)$$

$$-H_y^{cav}(M_1^x) - H_y^{cav}(M_1^y) + H_y^{cav}(M_2^x) + H_y^{cav}(M_2^y) + H_y^{cav}(M_3^x) + H_y^{wvg3}(M_2^x) + H_y^{cav}(M_3^y) + H_y^{wvg3}(M_3^y) = 0 \quad (18)$$

6. SOLVING FOR THE ELECTRIC FIELD

To determine the electric field distribution at the window aperture, it is necessary to determine the basis function coefficients $E_p^{i,x/y}$ at both the apertures. Since the each component of the field is described by M basis functions, 6M unknowns are to be determined from the boundary conditions. The Galerkin's specialization of the method of moments is used to obtain 6M-different equations from the boundary condition to enable determination of $E_p^{i,x/y}$ [10]. The weighting function $w_q^{i,x/y}(x, y, z)$ is selected to be of the same form as the basis function $e_p^{i,x/y}$. The weighting function is defined as follows:

$$w_q^{i,y} = \begin{cases} \sin\left\{\frac{q\pi}{2L}(x - x_w + L)\right\} & \text{for } x_w - L \leq x \leq x_w + L \\ 0 & \text{elsewhere} \end{cases} \quad (19a)$$

$$w_q^{i,x} = \begin{cases} \sin\left\{\frac{q\pi}{2W}(y - y_w + W)\right\} & \text{for } y_w - W \leq y \leq y_w + W \\ 0 & \text{elsewhere} \end{cases} \quad (19b)$$

The inner product is defined by

$$\langle H, w_q \rangle = \iint_{\text{Aperture}} H \cdot w_q d\xi d\psi \quad (20)$$

Using the boundary condition given by Equations (13) to (18) and the definition of Equation (20),

$$\langle \{H_x^{wvg1}(M_1^x) + H_x^{cav}(M_1^x)\}, w_q^{1,y} \rangle + \langle \{H_x^{wvg1}(M_1^y) + H_x^{cav}(M_1^y)\}, w_q^{1,y} \rangle - \langle H_x^{cav}(M_2^x), w_q^{1,y} \rangle - \langle H_x^{cav}(M_2^y), w_q^{1,y} \rangle - \langle H_x^{cav}(M_3^x), w_q^{1,y} \rangle - \langle H_x^{cav}(M_3^y), w_q^{1,y} \rangle = 2\langle H_x^{inc}, w_q^{1,x} \rangle \quad (21)$$

$$\langle \{H_y^{wvg1}(M_1^x) + H_y^{cav}(M_1^x)\}, w_q^{1,x} \rangle + \langle \{H_y^{wvg1}(M_1^y) + H_y^{cav}(M_1^y)\}, w_q^{1,x} \rangle - \langle H_y^{cav}(M_2^x), w_q^{1,x} \rangle - \langle H_y^{cav}(M_2^y), w_q^{1,x} \rangle - \langle H_y^{cav}(M_3^x), w_q^{1,x} \rangle - \langle H_y^{cav}(M_3^y), w_q^{1,x} \rangle = 0 \quad (22)$$

$$\begin{aligned}
& -\langle H_x^{cav}(M_1^x), w_q^{2,y} \rangle - \langle H_x^{cav}(M_1^y), w_q^{2,y} \rangle + \langle \{H_x^{cav}(M_2^x) + H_x^{wvg2}(M_2^x)\}, w_q^{2,y} \rangle \\
& + \langle \{H_x^{cav}(M_2^y) + H_x^{wvg2}(M_2^y)\}, w_q^{2,y} \rangle + \langle H_x^{cav}(M_3^x), w_q^{2,y} \rangle + \langle H_x^{cav}(M_3^y), w_q^{2,y} \rangle = 0 \quad (23)
\end{aligned}$$

$$\begin{aligned}
& -\langle H_y^{cav}(M_1^x), w_{qy,2} \rangle - \langle H_y^{cav}(M_1^y), w_q^{2,x} \rangle + \langle \{H_y^{cav}(M_2^x) + H_y^{wvg2}(M_2^x)\}, w_q^{2,x} \rangle \\
& + \langle \{H_y^{cav}(M_2^y) + H_y^{wvg2}(M_2^y)\}, w_q^{2,x} \rangle + \langle H_y^{cav}(M_3^x), w_q^{2,x} \rangle + \langle H_y^{cav}(M_3^y), w_q^{2,x} \rangle = 0 \quad (24)
\end{aligned}$$

$$\begin{aligned}
& -\langle H_x^{cav}(M_1^x), w_q^{3,y} \rangle - \langle H_x^{cav}(M_1^y), w_q^{3,y} \rangle + \langle H_x^{cav}(M_2^x), w_q^{3,y} \rangle + \langle H_x^{cav}(M_2^y), w_q^{3,y} \rangle \\
& + \langle \{H_x^{cav}(M_3^x) + H_x^{wvg3}(M_3^x)\}, w_q^{3,y} \rangle + \langle \{H_x^{cav}(M_3^y) + H_x^{wvg3}(M_3^y)\}, w_q^{3,y} \rangle = 0 \quad (25)
\end{aligned}$$

$$\begin{aligned}
& -\langle H_y^{cav}(M_1^x), w_q^{3,x} \rangle - \langle H_y^{cav}(M_1^y), w_q^{3,x} \rangle + \langle H_y^{cav}(M_2^x), w_q^{3,x} \rangle + \langle H_y^{cav}(M_2^y), w_q^{3,x} \rangle \\
& + \langle \{H_y^{cav}(M_3^x) + H_y^{wvg3}(M_3^x)\}, w_q^{3,x} \rangle + \langle \{H_y^{cav}(M_3^y) + H_y^{wvg3}(M_3^y)\}, w_q^{3,x} \rangle = 0 \quad (26)
\end{aligned}$$

where the elements of the moment matrices are derived as follows:

$$\langle H_x^{inc}, w_q^{1,y} \rangle = \begin{cases} -2abY_0 & \text{for } q = 1 \\ 0 & \text{Otherwise} \end{cases} \quad (27)$$

$$\langle H_x^{wvg}(M_x), w_q^{i,y} \rangle = \begin{cases} -2abY_{m0}^e & \text{for } p = q = m \text{ and } n = 0 \\ 0 & \text{Otherwise} \end{cases} \quad (28)$$

$$\langle H_x^{wvg}(M_y), w_q^{i,y} \rangle = 0 \quad (29)$$

$$\langle H_y^{wvg}(M_x), w_q^{i,x} \rangle = 0 \quad (30)$$

$$\langle H_y^{wvg}(M_y), w_q^{i,x} \rangle = \begin{cases} -2abY_{0n}^e & \text{for } p = q = n \text{ and } m = 0 \\ 0 & \text{Otherwise} \end{cases} \quad (31)$$

$$\begin{aligned}
\langle H_x^{cav}(M_x), w_q^{i,y} \rangle &= -\frac{j\omega\varepsilon L_s W_s L_o W_o}{k^2 2L_c W_c} \sum_{m=1}^{\infty} \sum_{n=0}^{\infty} \varepsilon_m \varepsilon_n \left\{ k^2 - \left(\frac{m\pi}{2L_c} \right)^2 \right\} \\
&\times \cos \left\{ \frac{n\pi}{2W_c} (y_{ws} + W_c) \right\} \sin c \left\{ \frac{n\pi}{2W_c} W_s \right\} \cos \left\{ \frac{n\pi}{2W_c} (y_{wo} + W_c) \right\} \sin c \left\{ \frac{n\pi}{2W_c} W_o \right\} \\
&\times \frac{\{-F_{xs}(p) F_{xo}(q)\}}{\Gamma_{mn} \sin \{2\Gamma_{mn} t_c\}} \begin{cases} \cos \{\Gamma_{mn}(z - t_c)\} \cos \{\Gamma_{mn}(z_0 + t_c)\} & z > z_0 \\ \cos \{\Gamma_{mn}(z_0 - t_c)\} \cos \{\Gamma_{mn}(z + t_c)\} & z < z_0 \end{cases} \quad (32)
\end{aligned}$$

$$\begin{aligned}
\langle H_x^{cav}(M_y), w_q^{i,y} \rangle &= \frac{j\omega\varepsilon L_s W_s L_o W_o}{k^2 2L_c W_c} \sum_{m=0}^{\infty} \sum_{n=1}^{\infty} \varepsilon_m \varepsilon_n \frac{m\pi}{2L_c} \frac{n\pi}{2W_c} \\
&\times \cos \left\{ \frac{m\pi}{2L_c} (x_{ws} + L_c) \right\} \sin c \left\{ \frac{m\pi}{2L_c} L_s \right\} \cos \left\{ \frac{n\pi}{2W_c} (y_{wo} + W_c) \right\} \sin c \left\{ \frac{n\pi}{2W_c} W_o \right\} \\
&\times \frac{\{-F_{ys}(p) F_{yo}(q)\}}{\Gamma_{mn} \sin \{2\Gamma_{mn} t_c\}} \begin{cases} \cos \{\Gamma_{mn}(z - t_c)\} \cos \{\Gamma_{mn}(z_0 + t_c)\} & z > z_0 \\ \cos \{\Gamma_{mn}(z_0 - t_c)\} \cos \{\Gamma_{mn}(z + t_c)\} & z < z_0 \end{cases} \quad (33)
\end{aligned}$$

$$\begin{aligned}
\langle H_y^{cav}(M_x), w_q^{i,x} \rangle &= \frac{j\omega\varepsilon L_s W_s L_o W_o}{k^2 2L_c W_c} \sum_{m=1}^{\infty} \sum_{n=0}^{\infty} \varepsilon_m \varepsilon_n \frac{m\pi}{2L_c} \frac{n\pi}{2W_c} \\
&\times \cos \left\{ \frac{m\pi}{2L_c} (x_{wo} + L_c) \right\} \sin c \left\{ \frac{m\pi}{2L_c} L_o \right\} \cos \left\{ \frac{n\pi}{2W_c} (y_{ws} + W_c) \right\} \sin c \left\{ \frac{n\pi}{2W_c} W_s \right\} \\
&\times \frac{\{-F_{xs}(p) F_{yo}(q)\}}{\Gamma_{mn} \sin \{2\Gamma_{mn} t_c\}} \begin{cases} \cos \{\Gamma_{mn}(z - t_c)\} \cos \{\Gamma_{mn}(z_0 + t_c)\} & z > z_0 \\ \cos \{\Gamma_{mn}(z_0 - t_c)\} \cos \{\Gamma_{mn}(z + t_c)\} & z < z_0 \end{cases} \quad (34)
\end{aligned}$$

$$\begin{aligned}
\langle H_y^{cav}(M_y), w_q^{i,x} \rangle &= -\frac{j\omega\varepsilon L_s W_s L_o W_o}{k^2 2L_c W_c} \sum_{m=0}^{\infty} \sum_{n=1}^{\infty} \varepsilon_m \varepsilon_n \left\{ k^2 - \left(\frac{n\pi}{2W_c} \right)^2 \right\} \\
&\times \cos \left\{ \frac{m\pi}{2L_c} (x_{ws} + L_c) \right\} \sin c \left\{ \frac{m\pi}{2L_c} L_s \right\} \cos \left\{ \frac{m\pi}{2L_c} (x_{wo} + L_c) \right\} \sin c \left\{ \frac{m\pi}{2L_c} L_o \right\} \\
&\times \frac{\{-F_{ys}(p) F_{yo}(q)\}}{\Gamma_{mn} \sin \{2\Gamma_{mn} t_c\}} \begin{cases} \cos \{\Gamma_{mn}(z - t_c)\} \cos \{\Gamma_{mn}(z_0 + t_c)\} & z > z_0 \\ \cos \{\Gamma_{mn}(z_0 - t_c)\} \cos \{\Gamma_{mn}(z + t_c)\} & z < z_0 \end{cases} \quad (35)
\end{aligned}$$

where suffix 's' and 'o' represents the source and observation aperture dimensions respectively.

Rewriting Equations (27) and (35) in the matrix form, for all p and q :

$$\begin{bmatrix}
 [Y_{11}^{xx}] & [Y_{11}^{xy}] & -[Y_{12}^{xx}] & -[Y_{12}^{xy}] & -[Y_{13}^{xx}] & -[Y_{13}^{xy}] \\
 [Y_{11}^{yx}] & [Y_{11}^{yy}] & -[Y_{12}^{yx}] & -[Y_{12}^{yy}] & -[Y_{13}^{yx}] & -[Y_{13}^{yy}] \\
 -[Y_{21}^{xx}] & -[Y_{21}^{xy}] & [Y_{22}^{xx}] & [Y_{22}^{xy}] & [Y_{23}^{xx}] & [Y_{23}^{xy}] \\
 -[Y_{21}^{yx}] & -[Y_{21}^{yy}] & [Y_{22}^{yx}] & [Y_{22}^{yy}] & [Y_{23}^{yx}] & [Y_{23}^{yy}] \\
 -[Y_{31}^{xx}] & -[Y_{31}^{xy}] & [Y_{32}^{xx}] & [Y_{32}^{xy}] & [Y_{33}^{xx}] & [Y_{33}^{xy}] \\
 -[Y_{31}^{yx}] & -[Y_{31}^{yy}] & [Y_{32}^{yx}] & [Y_{32}^{yy}] & [Y_{33}^{yx}] & [Y_{33}^{yy}]
 \end{bmatrix}
 \begin{Bmatrix}
 \{E^{1,y}\} \\
 \{E^{1,x}\} \\
 \{E^{2,y}\} \\
 \{E^{2,x}\} \\
 \{E^{3,y}\} \\
 \{E^{3,x}\}
 \end{Bmatrix}
 =
 \begin{Bmatrix}
 2\{h_x^{inc}\} \\
 \{0\} \\
 \{0\} \\
 \{0\} \\
 \{0\} \\
 \{0\}
 \end{Bmatrix}
 \quad (36)$$



Figure 3: Photograph of arrangements of H -plane bends for measurement purpose.

7. REFLECTION COEFFICIENT AND TRANSMISSION COEFFICIENT

The procedure for derivation of reflection and transmission coefficients is given in [11]. Following the same procedure the expressions for Γ and T is given by:

$$\Gamma = \frac{E_y^1 + E_y^2}{E_y^{inc}} = -1 - E_1^{1,y} \quad (37)$$

$$T_{21/31} = \frac{E_y^{transmitted}}{E_y^{inc}} = -E_1^{2/3,y} \quad (38)$$

8. NUMERICAL RESULTS AND DISCUSSION

Theoretical data for the magnitude of scattering parameters for an H -plane 1:2 WR-90 waveguide power divider at X-band has been compared with CST Microwave Studio simulated data and measured data in Figure 4.

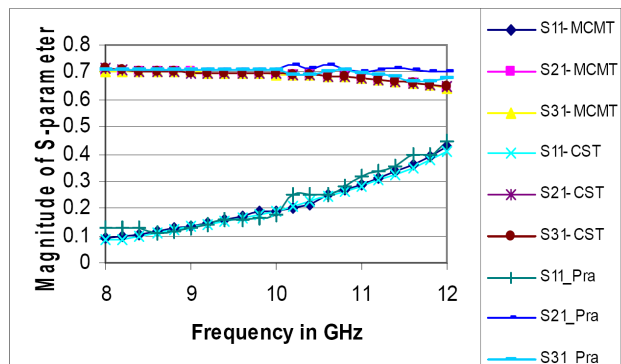


Figure 4: Comparison of theoretical, CST microwave studio simulated and measured data for an H -plane 1:2 WR-90 waveguide power divider for $2t = 12.2$ mm.

MATLAB codes have been written for analyzing the structure and numerical data have been obtained after running the codes. The structure was also simulated using CST microwave studio while measurements were performed using Agilent 8410C Vector Network Analyzer. The theory has been validated by the excellent agreement between the theoretical, CST Microwave Studio simulated data and Measured Data in Figure 4. In Figure 5, S_{11} is presented for various values of the length of cavity ($2t$) and in Figure 6 for S_{21} and S_{31} . The scattering parameters for the circuit, when excited through port -2 and port -3 have not been presented in this section because these are less important in the study of a power divider.

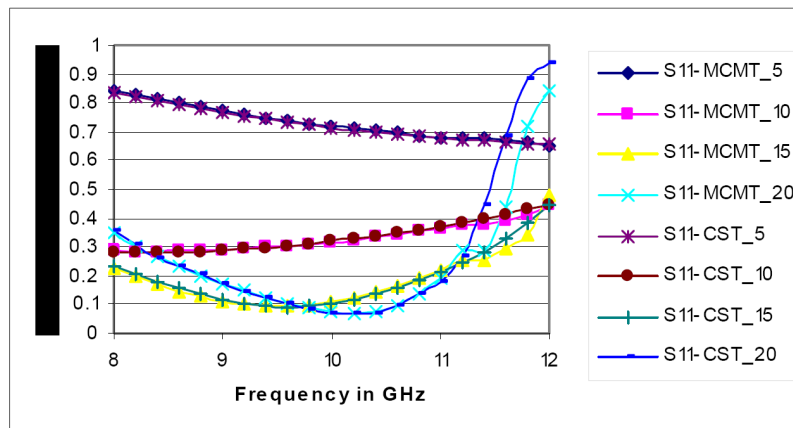


Figure 5: S_{11} of an H -plane 2:1 WR-90 waveguide power divider with $2t = 5$ mm, 10 mm, 15 mm and 20 mm.

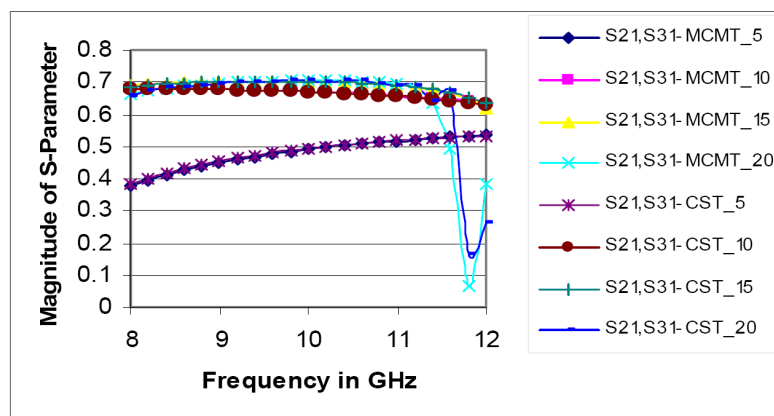


Figure 6: S_{21} and S_{31} of an H -plane 2:1 WR-90 waveguide power divider with $2t = 5$ mm, 10 mm, 15 mm, and 20 mm.

ACKNOWLEDGMENT

The support provided by Kalpana Chawla Space Technology Cell, IIT Kharagpur is gratefully acknowledged.

REFERENCES

1. Takeda, F., O. Ishida, and Y. Isoda, "Waveguide power divider using metallic septum with resistive coupling slot," *Microwave Symposium Digest, MTT-S International*, Vol. 82, No. 1, 527–528, June 1982.
2. Soroka, A. S., A. O. Silin, V. I. Tkachenko, and I. S. Tsakanyan, "Simulation of multichannel waveguide power dividers," *MSMW'98 Symposium Proceedings*, 634–635, Kharkov, Ukraine, September 15–17, 1998.
3. Chen, S., "A radial waveguide power divider for Ka band phase array antenna," *3rd International Conference on Microwave and Millimeter Wave Technology*, 948–951, 2002.

4. Gardner, P. and B. H. Ong, “Mode matching design of three-way waveguide power dividers,” *IEE Colloquium on Advances in Passive Microwave Components*, 5/1–5/4, May 22, 1997.
5. Das, S. and A. Chakrabarty, “Analysis of waveguide based power divider using multiple cavity modeling technique and performance improvement,” *IRSI-2005*, Bangalore, India.
6. Panda, D. K. and A. Chakraborty, “Multiple cavity modeling of a feed network for two dimensional phased array application,” *Progress In Electromagnetics Research Letters*, Vol. 2, 135–140, 2008.
7. Das, S. and A. Chakraborty, “A novel modeling technique to solve a class of rectangular waveguide based circuits and radiators,” *Progress In Electromagnetic Research*, PIER 61, 231–252, MIT, USA, May 2006.
8. Harrington, R. F., *Time-harmonic Electromagnetic Fields*, McGraw-Hill Book Company, New York, 1961.
9. Collins, R. E., *Field Theory of Guided Waves*, IEEE Press, 1991.
10. Harrington, R. F., *Field Computation by Moment Methods*, Roger E. Krieger Publishing Company, USA.
11. Das, S., “Analysis of rectangular waveguide based passive devices and antennas using multiple cavity modeling technique,” PhD Dissertation, Department of E & ECE, I. I. T Kharagpur, India, 2007.